Cabozantinib based combination therapy for the treatment of Hepatocellular Carcinoma

Runze Shang, Xinhua Song, Pan Wang, Yi Zhou, Xinjun Lu, Jingxiao Wang, Meng Xu, Xinyan Chen, Kirsten Utpatel, Li Che, Binyong Liang, Antonio Cigliano, Matthias Evert, Diego F. Calvisi , and Xin Chen

Table of contents

Supplementary Materials and methods

Human Liver Tissue Specimens

A collection of 64 formalin-fixed, paraffin-embedded HCC samples was used in the present study. HCC specimens were collected at the Institute of Pathology of the University of Regensburg (Regensburg, Germany). Institutional Review Board approval was obtained at the local Ethical Committee of the Medical University of Regensburg (approval # 17-1015-101). Informed consent was obtained from all individuals. Investigation has been conducted in accordance with the ethical standards and the Declaration of Helsinki.

Human TCGA analysis

Protein normalized expression data was acquired from Broad Institute GDAC Firehose (http://gdac.broadinstitute.org/), with 184 human HCC samples. All analyses were conducted with R (version 3.6.3). AKT/mTOR pathway activation was calculated with the mean of p-AKT S473, p-AKT T308, p-mTOR, p-S6 S235-S236, p-S6 S240-S244, and p-70S6K T389. AKT/mTOR and p-MET values >0 are considered to be activated or high; and values <0 are considered to be inactivated or low. Heatmap and annotation was drawn with Complex Heatmap.

Plasmids and reagents

The plasmids used in this study, including pT3-EF1α-c-Met (human c-Met or hMet), pT3-EF1α-ΔN90-β-Catenin, pT3EF1α-c-Myc, pT3-EF1α-HA-myr-AKT, pT2CAGGS-NRasV12 and pCMV/sleeping beauty transposase (SB), have been described previously (1-3). All plasmids were purified by using the Endotoxin free Maxi Prep Kit (Sigma-Aldrich, St. Louis, MO) before injection. Cabozantinib and MLN0128 were purchased from LC Laboratories (Woburn, MA). Anti-mouse PD-L1 Ab was provided

by Genetech, Inc. (South San Francisco, CA), while control IgG was purchased from BioXcell (West Lebanon, NH).

Hydrodynamic injection and mouse treatment

Female wild-type FVB/N mice were obtained from Charles River Laboratories (Wilmington, MA). Sleeping beauty (SB)-mediated hydrodynamic injection was performed as previously described (4). To generate the c-Met/β-Catenin HCC model, 20μg pT3-EF1α-c-Met plasmids (human) and 20μg pT3-EF1α-ΔN90-β-Catenin plasmids along with 1.6μg pCMV/SB in 2ml of normal saline (0.9%NaCl) were hydrodynamically injected into the tail vein of 6- to 8-week-old mice. To establish the Akt/c-Met HCC murine model, mice received 20μg pT3-EF1α-HA-myr-AKT plasmids mixed with 20μg pT3-EF1α-c-Met plasmids (human) along with 1.6μg pCMV/SB in 2ml of normal saline (0.9%NaCl). To induce the c-Myc HCC mouse model, mice received 20μg pT3EF1α-c-Myc plasmids mixed with 0.8μg pCMV/SB in 2ml of normal saline (0.9%NaCl). For the generation of the Akt/Ras HCC model, 20μg pT3-EF1α-HA-myr-AKT plasmids mixed 20μg pT2CAGGS-NRasV12 plasmids mixed with 1.6μg pCMV/SB in 2ml of normal saline (0.9%NaCl) were hydrodynamically injected into the tail vein of mice. Cabozantinib (60mg/kg/day), MLN0128 (1.0mg/kg/day), Cabozantinib (60mg/kg/day) + MLN0128 (0.5mg/kg/day) or vehicle was orally administered via gavage. Anti-mouse PD-L1 Ab (or isotype IgG) was intraperitoneally injected twice a week for three weeks. Therapy administration was performed 3.5 (Akt/Ras HCC model) or 5.5 weeks (c-Met/β-Catenin, Akt/c-Met and c-Myc HCC model) post injection for 3 consecutive weeks. Mice were housed, fed, and monitored in accord with protocols approved by the Committee for Animal Research at the University of California San Francisco (San Francisco, CA). The abdominal girth and the signs of morbidity or discomfort were monitored for all mice. Mice were sacrificed at indicated time points

or when they developed high liver tumor burden, i.e., mice showed abdominal swelling, which correlated to liver weight greater than 5g, and the mice were considered to be "deceased" per our IACUC protocol. Liver weight and liver tumor size were measured for each mouse.

Biochemical assays

The serum alanine aminotransferase (ALT), aspartate aminotransferase (AST), alkaline phosphatase (ALKP), total protein (TP), and albumin (ALB) levels were assayed using standard clinical protocol by the Clinical Laboratory at Zuckerberg San Francisco General Hospital (San Francisco, CA).

Flow cytometric analysis

Single-cell suspensions of lymphocytes from spleen and liver/tumors were stained with fluorochrome-labeled antibodies (Supplementary table) as described (5, 6). Cells were analyzed with the LSR II cytometer (BD Biosciences, San Jose, CA). Data were analyzed by the FlowJo software (LLC, Ashland, OR).

Immunohistochemistry (IHC), Sirius Red staining, and senescence assay

Parts of liver specimens were fixed in 4% paraformaldehyde overnight at 4°C and then embedded in paraffin, whereas other liver tissues were frozen in Tissue-Tek OCT compound (Sakura Finetek USA, Inc., Torrance, CA) using a bath of 2-methylbutane (Thermo Fisher Scientific, Pittsburgh, PA) cooled on dry ice. Tissue sections were cut from paraffin or frozen blocks at 5 μm in thickness.

For immunohistochemical staining, the slides were deparaffinized and then microwaved in 10 mmol/L citrate buffer (pH 6.0) for 10 minutes for antigen retrieval.

After 20 minutes cool down at room temperature, the slides were blocked using 5% goat serum and Avidin-Biotin blocking kit (Vector Laboratories, Burlingame, CA). Subsequently, the slides were incubated with primary antibodies (Supplementary Table 1) overnight at 4°C. The immunoreactivity was visualized with the Vectastain Elite ABC kit (Vector Laboratories, Burlingame, CA), using Vector NovaRED™ (Vector Laboratories) as the chromogen. Slides were then counterstained with hematoxylin solution (ThermoFisher Scientific, Pittsburg, PA). Apoptosis index was determined in mouse HCC lesions by counting TUNEL positive cells on at least 2000 tumor cells per mouse using the TumorTACS™ In Situ Apoptosis Detection Kit (Trevigen, Gaithersburg, MD), in accordance with the manufacturer's protocol.

For the Sirius Red staining, tissue sections were heated at 60°C for 45 min and then deparaffinized. After incubated with a Picro-Sirius Red stain solution (0.1% direct red 80 plus 0.1% fast green FCF dissolved in saturated aqueous picric acid) for 60 mins, the sections were dehydrated.

For cellular senescence assay, the Cellular Senescence Assay kit (EMD Millipore, Billerica, MA) was used. Briefly, sections from frozen blocks were fixed and stained with SA-β-gal staining solution for 4 hours. The resulting images were viewed under light microscopy.

Protein extraction and Western blot analysis

Mouse liver tissues and cells were homogenized in M-PER™ Mammalian Protein Extraction Reagent (ThermoFisher Scientific) containing the Halt™ Protease Inhibitor Cocktail (ThermoFisher Scientific). Next, protein concentrations were determined with the Pierce™ Microplate BCA Protein Assay Kit (ThermoFisher Scientific). For Western blotting, extracted proteins were boiled in Tris-Glycine SDS Sample Buffer (Bio-Rad) for denaturation and subsequently separated by SDS-PAGE, and transferred onto

nitrocellulose membranes (Bio-Rad). Membranes were blocked in 10% non-fat milk in Tris-buffered saline containing 0.05% Tween-20 for 1 hour at room temperature and then incubated with primary antibodies (summarized in Supplementary Table 2) at 4°C overnight. Membranes were then incubated with horseradish peroxidase-secondary antibody (1:5000; Jackson ImmunoResearch Laboratories Inc., West Grove, PA) at room temperature for 1 hour. After appropriate washing, membranes were developed with the Super Signal West Dura Kit (ThermoFisher Scientific, Waltham, MA).

In *vitro* experiments

Thirteen HCC cell lines (HLE, PLC/PRF/5, SNU-449, Huh7, SNU-475, SNU-387, MHCC97-H, Hep3B, HLF, SNU-182, SNU-423, Focus, and Hep40) and 1 human hepatoblastoma cell line (HepG2) were used in this study. HLE, PLC/PRF/5, Huh7, MHCC97-H, Hep3B, HLF, Focus, Hep40 and HepG2 cell lines were cultured in Dulbecco's modified Eagle medium (DMEM) supplemented with 10% FBS, penicillin (100 U/mL), and streptomycin (100 μg/mL). SNU-449, SNU-475, SNU-387, SNU-182 and SNU-423 cells were maintained in Roswell Park Memorial Institute 1640 (RPMI 1640) medium supplemented with 10% FBS, penicillin (100 U/mL), and streptomycin (100 μg/mL). All cell lines were cultured at 37°C in an atmosphere of humidified air containing 5% CO2. For IC_{50} determination, cells were seeded in 24-well plates and treated with gradient concentration of Cabozantinib in triplicate for 48 hours. Then cells were enumerated by crystal violet staining. After washing, stained cells were incubated in lysis solution and shaken gently on a rocking shaker for 20–30 min. Diluted lysate solutions were added to 96-well plates and OD was measured at 590 nm with the BioTek ELX808 Absorbance Microplate Reader (ThermoFisher Scientific). For the BrdU incorporation assay, control or drug-treated cells were incubated with bromodeoxyuridine (BrdU) for 1 h and the assay was performed using the FITC BrdU

Flow Kit (BD Biosciences, San Jose, CA), following the manufacturer's instructions. The measurement of cell cycle parameters was performed with the Becton Dickinson LSRII Flow Cytometer (BD Biosciences) and the data processed using the FlowJo 10 (LLC). Cell proliferation was assessed in MHCC97-H and HLE HCC cell lines at the 24- and 48-hour time points using the BrdU Cell Proliferation Assay Kit (Cell Signaling Technology, Danvers, MA). As concerns apoptosis, it was determined in the two HCC cell lines using the Cell Death Detection Elisa plus Kit (Roche Molecular Biochemicals, Indianapolis, IN, USA), following the manufacturer' instructions. DMSO-, and Cabozantinib-treated cells were initially subjected to 24h serum starvation. Subsequently, apoptotic cell death was assessed at 24h and 48h time points. All experiments were repeated at least three times in triplicate.

Combination index

The combinatory index (CI) of Cabozantinib and MLN0128 was calculated by the Chou–Talalay method as previously described (7). Briefly, HCC cells were treated with various doses of Cabozantinib and/or MLN0128. Then the CI was calculated, where CI<1, =1, and >1 indicates synergistic effect, additive effect and antagonism, respectively.

Assessment of cholesterol, triglycerides, and glucose uptake levels

Total cholesterol and triglyceride levels in MHCC97-H and HLE cell lines were assessed using the Cholesterol Quantitation Kit and the Triglyceride Quantification Kit (BioVision Inc., Mountain View, CA, USA), respectively, following the manufacturer's recommendation. Glucose uptake was determined in the same cells using the Glucose

Uptake-Glo™ Assay (Promega, Madison, WI) according to the manufacturer's instructions.

Statistical analysis

GraphPad Prism 6.0 (GraphPad Software Inc.) was used to analyze the data. Statistical analyses were conducted using Student's t-test, Tukey-Kramer test and linear regression analyses. The data were presented as Means±SD. Values of $P<0.05$ were considered statistically significant.

References

1. Wang C, Cigliano A, Jiang L, Li X, Fan B, Pilo MG*, et al*. 4EBP1/eIF4E and p70S6K/RPS6 axes play critical and distinct roles in hepatocarcinogenesis driven by AKT and N-Ras proto-oncogenes in mice. Hepatology 2015;61(1):200-13.
2. Liu P, Ge M, Hu J, Li X, Che L, Sun K*, et al*. A functional mammalian target of rapamycin complex 1 signaling is indispensable for c-Myc-driven hepatocarcinogenesis. Hepatology 2017;66(1):167-81.
3. Qiao Y, Wang J, Karagoz E, Liang B, Song X, Shang R*, et al*. Axis inhibition protein 1 (Axin1) Deletion-Induced Hepatocarcinogenesis Requires Intact beta-Catenin but Not Notch Cascade in Mice. Hepatology 2019;70(6):2003-17.
4. Tward AD, Jones KD, Yant S, Cheung ST, Fan ST, Chen X*, et al*. Distinct pathways of genomic progression to benign and malignant tumors of the liver. Proc Natl Acad Sci U S A 2007;104(37):14771-6.
5. Avella DM, Li G, Schell TD, Liu D, Zhang SS, Lou X*, et al*. Regression of established hepatocellular carcinoma is induced by chemoimmunotherapy in an orthotopic murine model. Hepatology 2012;55(1):141-52.
6. Burch TK, Luchstead EF. Functional obstructive cardiomyopathy. Familial idiopathic hypertrophic subaortic stenosis in children. J Kans Med Soc 1973;74(9):335-8.
7. Song X, Liu X, Wang H, Wang J, Qiao Y, Cigliano A*, et al*. Combined CDK4/6 and Pan-mTOR Inhibition Is Synergistic Against Intrahepatic Cholangiocarcinoma. Clinical Cancer Research 2019;25(1):403-13.

Supplementary Figures

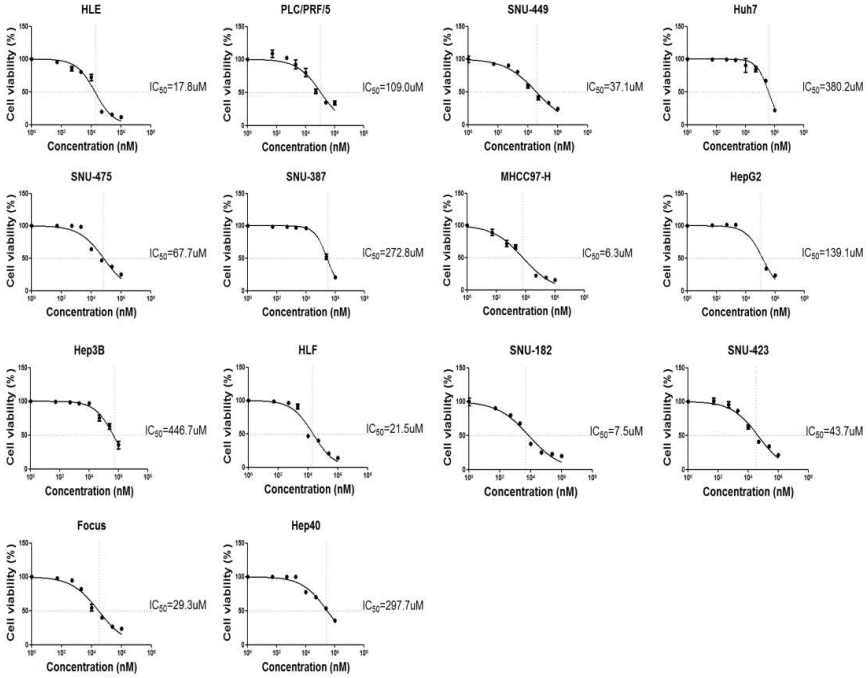

Supplementary Figure 1. Cabozantinib inhibits the proliferation of HCC cell lines.

Fourteen cell lines were treated with escalating concentrations of Cabozantinib for 48 hours, and IC_{50} values were calculated.

A

Cell line	MHCC97-H	SNU-182	HLE	HLF	Focus	SNU-449	SNU-423	SNU-475	PLC/PRF/5	HepG2	SNU-387	Hep40	Huh7	Hep3B
IC_{50} (μmol/L)	6.3	7.5	17.8	21.5	29.3	37.1	43.7	67.7	109.0	139.1	272.8	297.7	380.2	446.7

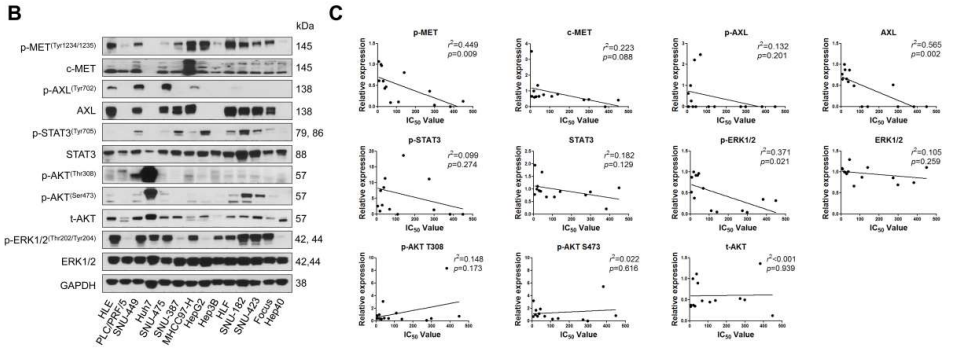

Supplementary Figure 2. Cabozantinib inhibits HCC growth *in vitro*. (A) IC_{50} values of 14 HCC cell lines were listed in the table. **(B)** Protein levels of phosphorylated/activated AXL, phosphorylated/activated c-MET and its downstream effectors (STAT3, AKT, and ERK) were assessed in 14 HCC cell lines by Western blot analysis. **(C)** Correlation between relative protein expression and IC_{50} values of different cell lines was analyzed by Pearson correlation method. Abbreviations: p, phosphorylated; t, total.

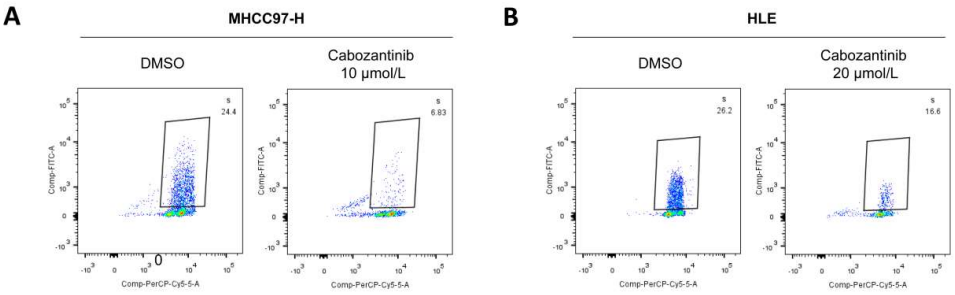

Supplementary Figure 3. Effects of Cabozantinib treatment on cell cycle of HCC cells. Cabozantinib treatment enhanced cell cycle arrest in MHCC97-H (A) and HLE (B) cell lines.

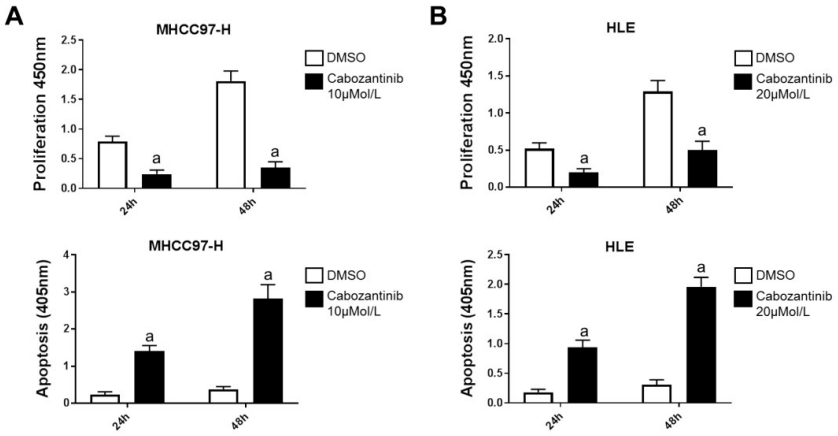

Supplementary Figure 4. Effect of Cabozantinib on proliferation and apoptosis of HCC cell lines. Reduced proliferation was detected in MHCC97-H (**A**; upper panel) and HLE (**B**; upper panel) cell lines following treatment with Cabozantinib when compared to solvent (DMSO). Apoptosis was significantly enhanced in MHCC97-H (**A**; lower panel) and HLE (**B**; lower panel) cell lines in Cabozantinib-treated cells. Each bar represents mean ± SD of three independent experiments conducted in triplicate. Mann-Whitney test: $P < 0.0001$; a, vs. DMSO.

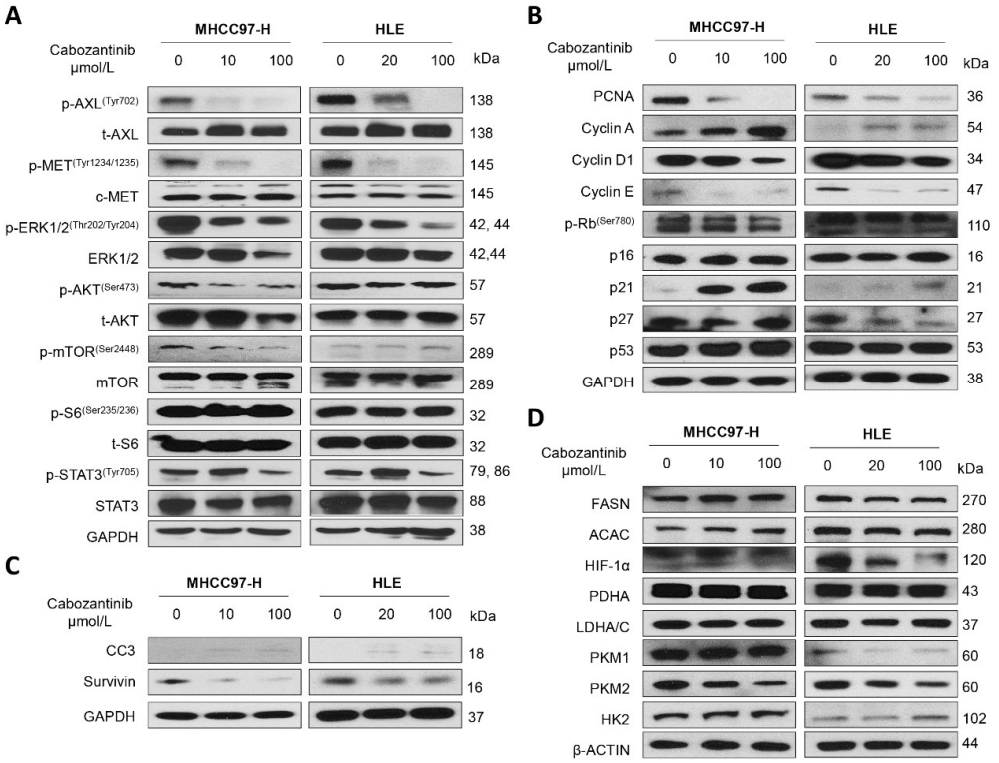

Supplementary Figure 5. Western blot analysis of potential targets of Cabozantinib in MHCC97-H and HLE human HCC cell lines. **(A)** Representative Western blot analysis of phosphorylated AXL, phosphorylated MET and downstream components in the c-MET cascade in MHCC97-H and HLE cell lines after treatment with indicated doses of Cabozantinib. Representative Western blot analysis of proliferation **(B)**, apoptosis **(C)**, lipogenic and glycolysis **(D)** pathways in MHCC97-H and HLE cell lines after treatment with indicated doses of Cabozantinib. Abbreviations: p, phosphorylated; t, total; CC3, cleaved caspase-3.

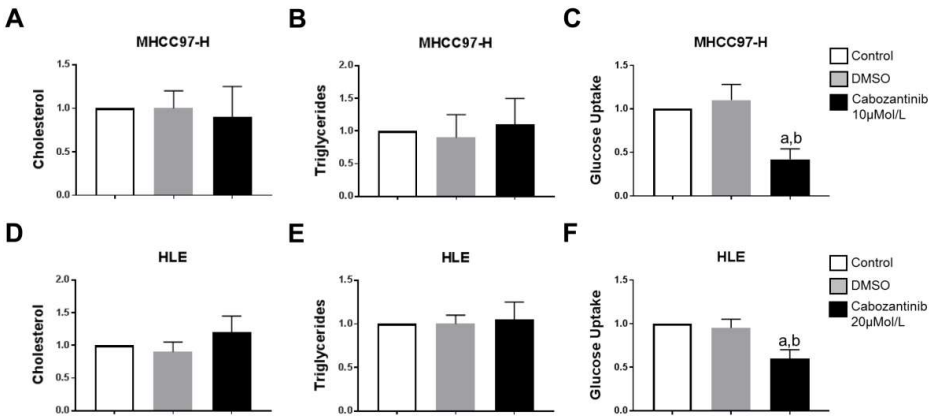

Supplementary Figure 6. Effect of Cabozantinib on lipogenesis and glycolysis in HCC cell lines. While no effects of the levels of cholesterol and triglycerides accompanied Cabozantinib administration in the two cell lines **(A, B, D and E)**, the glucose uptake (a marker of glycolysis) was significantly reduced in MHCC7-H **(C)** and HLE **(F)** cell lines following treatment with Cabozantinib when compared to control (untreated cells) and solvent alone (DMSO). Each bar represents mean ± SD of three independent experiments conducted in triplicate. Tukey-Kramer test: $P < 0.01$; a, vs. control; b, vs DMSO.

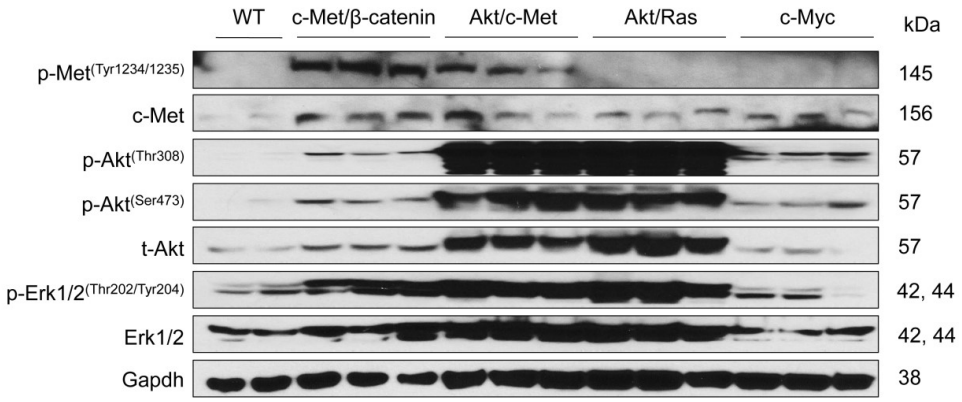

Supplementary Figure 7. High levels of phosphorylated/activated (p-)Met may be a useful biomarker to predict favorable response to Cabozantinib treatment in mouse models of HCC. Western blot analysis was performed to analyze the relative protein expression of components of the c-Met signaling cascade from wild-type FVB/N, late stage c-Met/β-Catenin, Akt/c-Met, Akt/Ras and c-Myc mouse liver tumor samples. Abbreviations: WT, wild-type; p, phosphorylated; t, total.

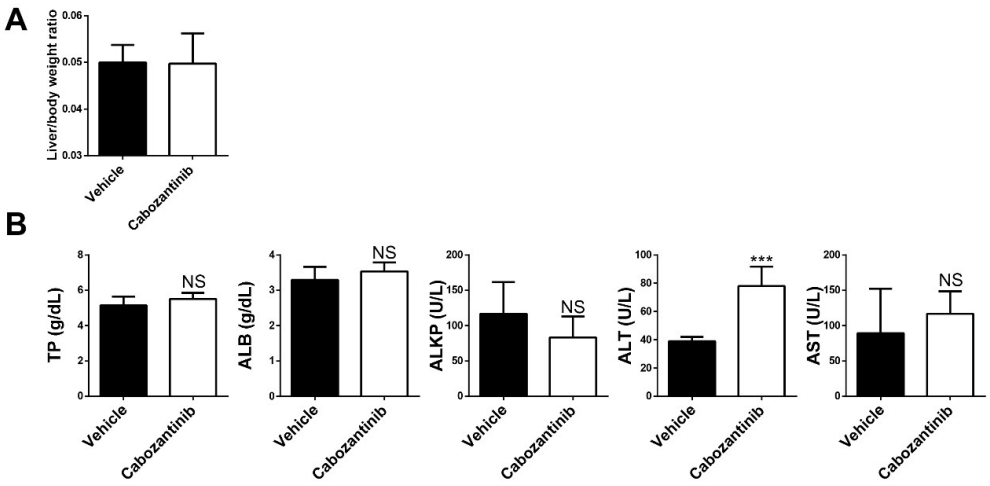

Supplementary Figure 8. Toxicity of Cabozantinib treatment in FVB/N mice. (A) Liver/body weight ratio of Vehicle- or Cabozantinib-treated FVB/N mice. **(B)** Indicators of liver function in FVB/N mice treated with Vehicle or Cabozantinib. Abbreviations: ALT, alanine aminotransferase; AST, aspartate aminotransferase; TBIL, total bilirubin; DBIL, direct bilirubin; TP, total protein; ALB, albumin. At least 3 mice per group were analyzed. Tukey–Kramer test: at least $P < 0.05$.

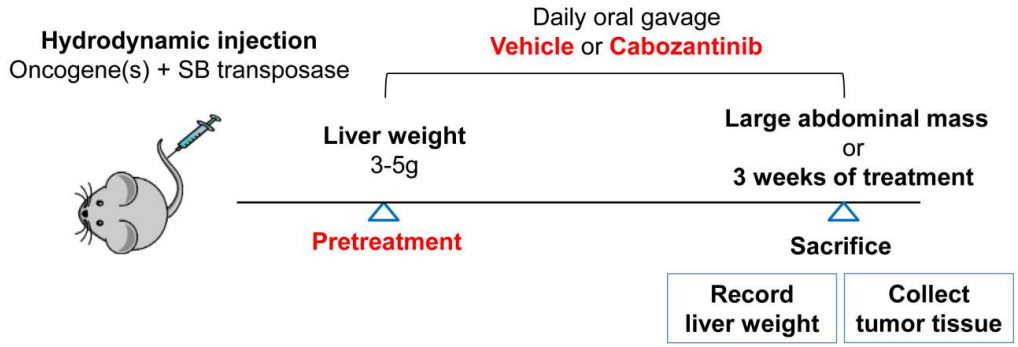

Supplementary Figure 9. Scheme of *in vivo* experiments. Mice were hydrodynamically injected with plasmids encoding the oncogene(s) and SB transposase plasmids. Mice were randomly separated into pretreatment, vehicle-, and Cabozantinib-treated groups. Mice in pretreatment cohort were harvested when their liver weight reached 3 to 5g. Mice in vehicle or Cabozantinib cohorts were sacrificed if they developed large abdominal mass or after 3 weeks of treatment.

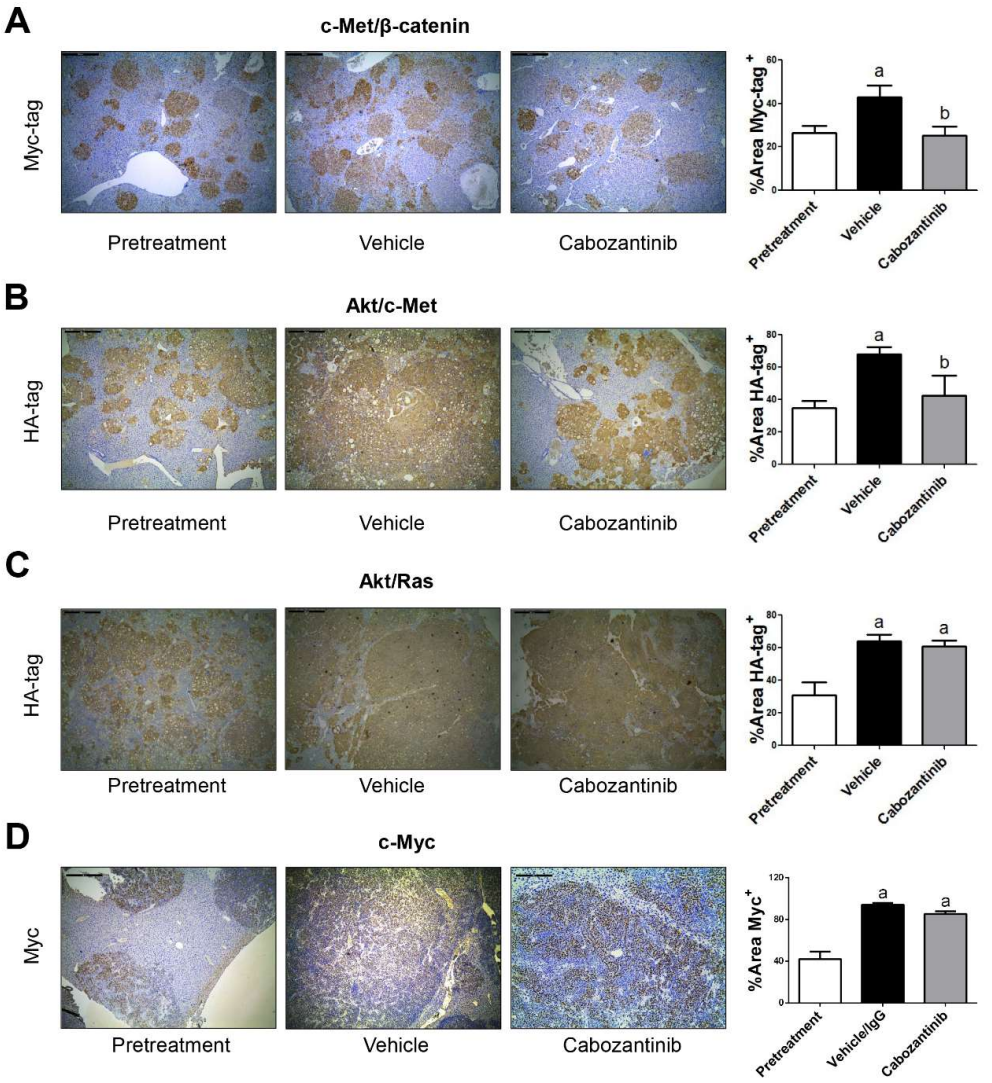

Supplementary Figure 10. Cabozantinib suppresses tumor growth in c-Met/β-catenin and Akt/c-Met mouse HCC. (A) Myc-tag (magnification ×40; scale bar =500 μm) staining in livers from c-Met/β-Catenin mice. **(B and C)** HA-tag (magnification ×40; scale bar =500 μm) staining in livers from Akt/c-Met and Akt/Ras mice. **(D)** Myc (magnification ×40; scale bar =500 μm) staining in livers from c-Myc mice.

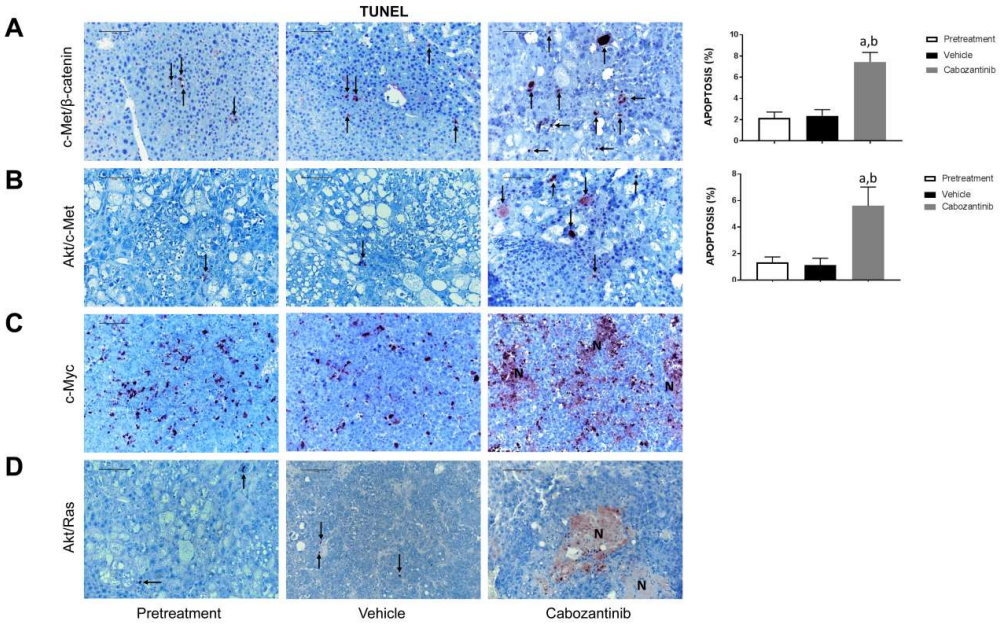

Supplementary Figure 11. Cabozantinib induces apoptosis and necrosis in HCC from different mouse models. TUNEL staining (magnification ×200; scale bar =100 μm) of liver lesions from c-Met/β-Catenin **(A)**, Akt/c-Met **(B)**, c-Myc **(C)** and Akt/Ras **(D)** mice. While in c-Met/β-Catenin and Akt/c-Met mouse tumors Cabozantinib treatment significantly increased apoptosis, a proper assessment of this parameter was difficult in c-Myc and AKT/Ras mice, where large areas of the tumors were replaced by necrosis (N) following Cabozantinib administration. Arrows indicate apoptotic cells. Student's *t* test: $P < 0.001$; a, vs. Pretreatment; b, vs. Vehicle.

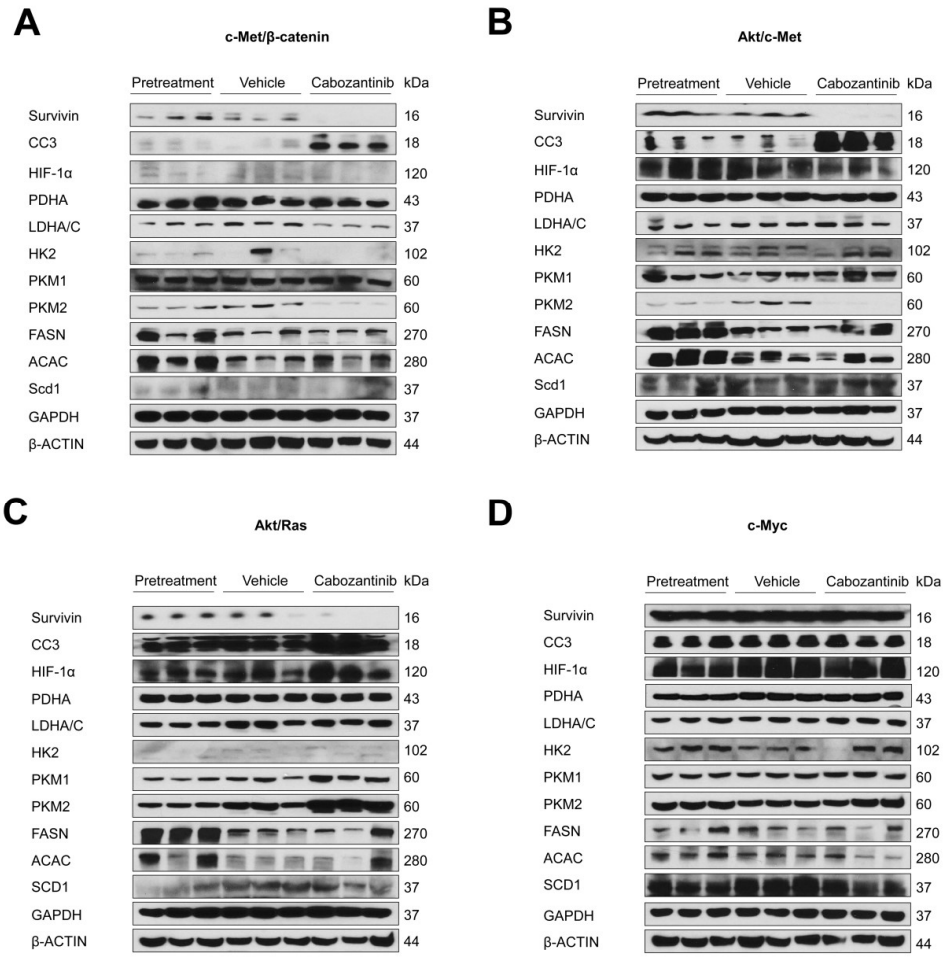

Supplementary Figure 12. Western blot analysis of additional potential targets of Cabozantinib in c-Met/β-Catenin mice. (A), **Akt/c-Met mice (B), Akt/Ras mice (C), and c-Myc mice (D).** Abbreviations: p, phosphorylated, CC3, cleaved caspase 3.

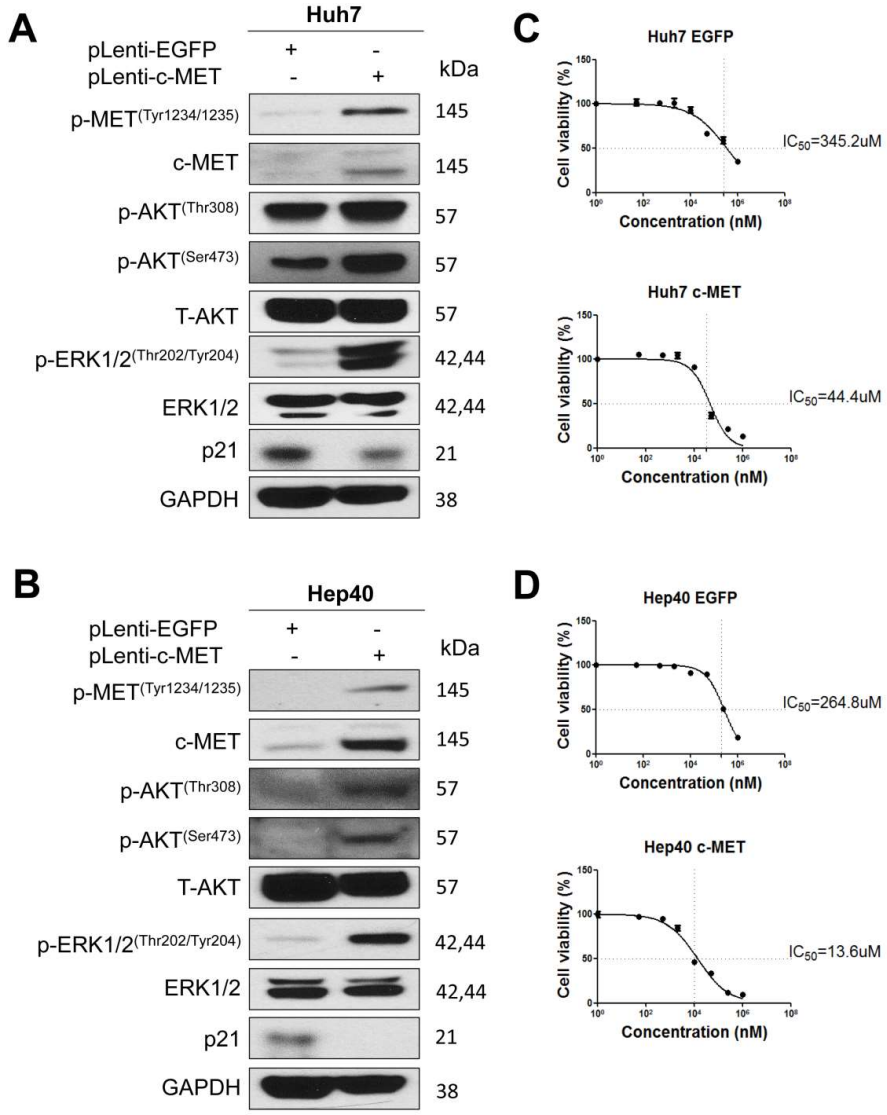

Supplementary Figure 13. Induction of c-MET increases the sensitivity to Cabozantinib treatment of HCC cells. Induction of c-MET proto-oncogene and its downstream effectors by lentivirus in Huh7 **(A)** and Hep40 **(B)** cell lines was confirmed by Western blot analysis. Huh7 and Hep40 cell lines were treated with escalating concentrations of Cabozantinib for 48 hours after the transfection of pLenti-EGFP and plenti-c-MET, and IC_{50} values were calculated (**C** and **D**).

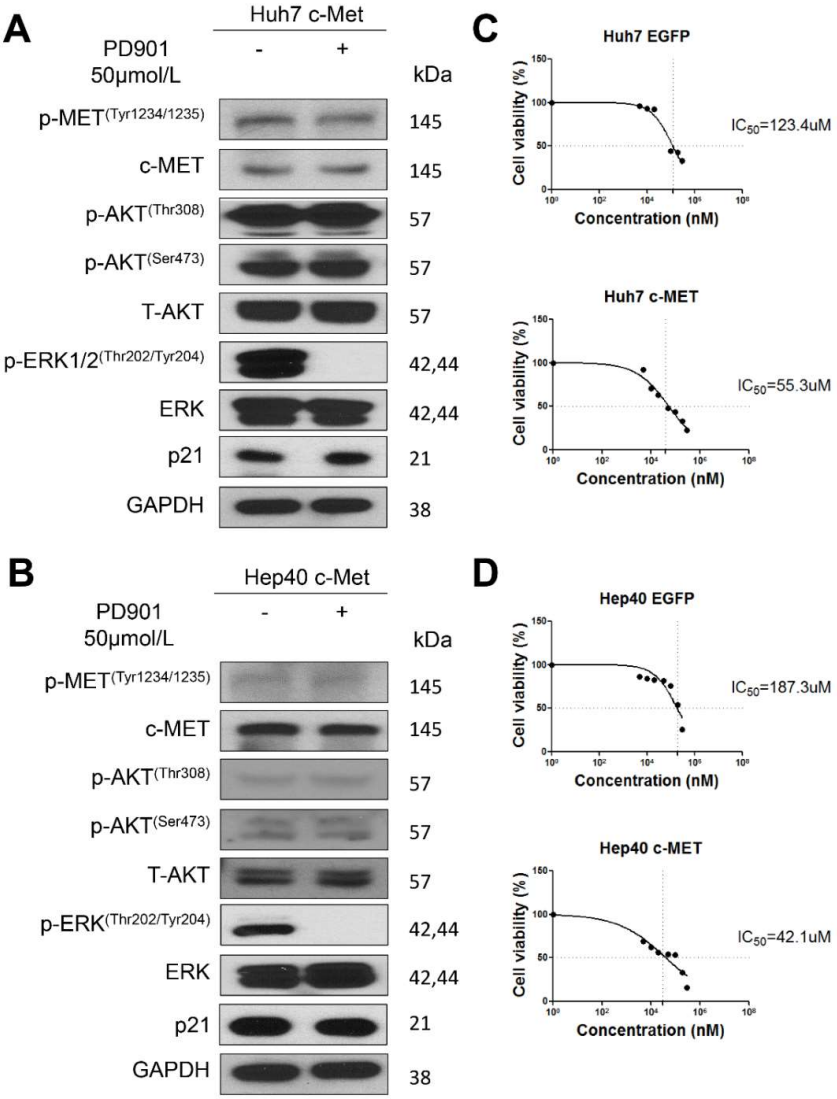

Supplementary Figure 14. Induction of c-MET increases the sensitivity of HCC cells to the MEK inhibitor PD091. Effects of PD901 on c-MET proto-oncogene and its downstream effectors in Huh7 **(A)** and Hep40 **(B)** cell lines were assessed by Western blot analysis. Huh7 and Hep40 cell lines were treated with escalating concentrations of PD901 for 48 hours after the transfection of pLenti-EGFP and plenti-c-MET, and IC_{50} values were calculated **(C and D)**.

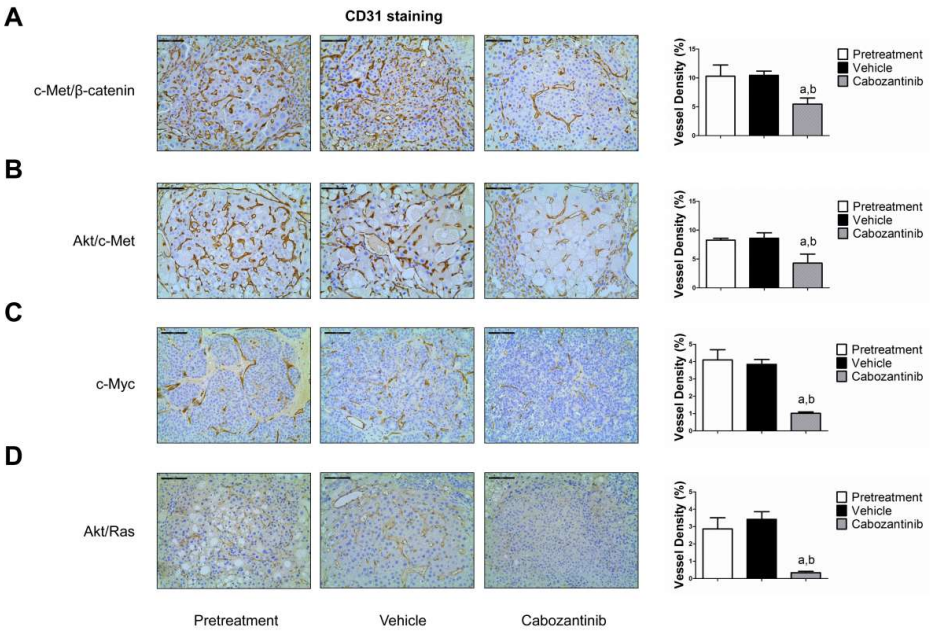

Supplementary Figure 15. Cabozantinib inhibits angiogenesis in HCC from different mouse models. CD31 (magnification ×200; scale bar =100 μm) staining in livers from c-Met/β-Catenin **(A)**, Akt/c-Met **(B)**, c-Myc **(C)**, and Akt/Ras **(D)** mice. Student's t test: at least $P < 0.05$; a, vs. Pretreatment; b, vs. Vehicle.

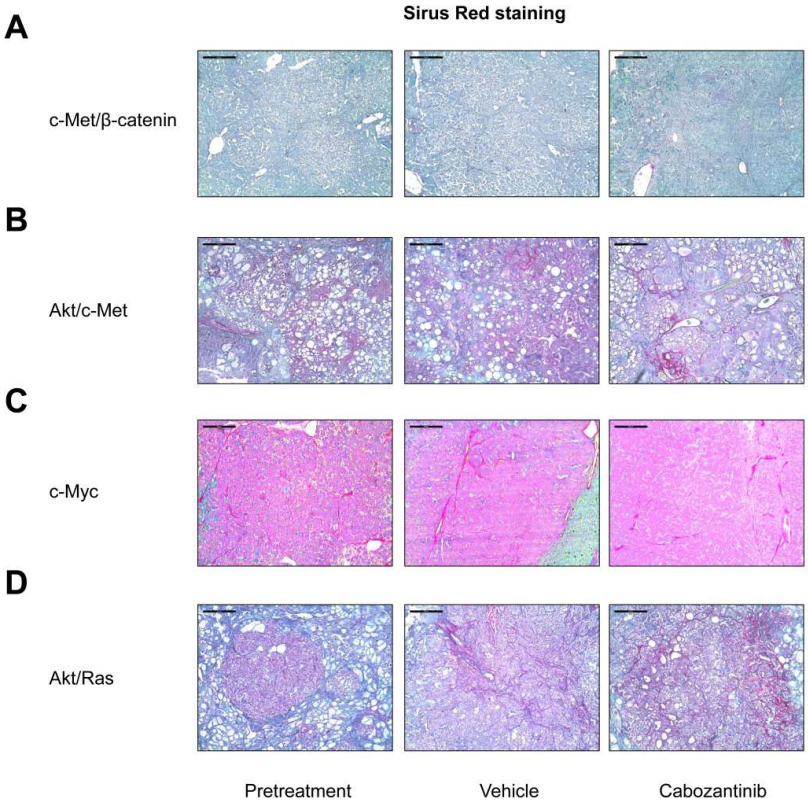

Supplementary Figure 16. Cabozantinib treatment does not affect cancer associated fibrosis in mouse HCCs. Sirius Red (magnification ×100; scale bar =200 μm) staining in livers from c-Met/β-Catenin **(A)**, Akt/c-Met **(B)**, c-Myc **(C)** and Akt/Ras **(D)** mice.

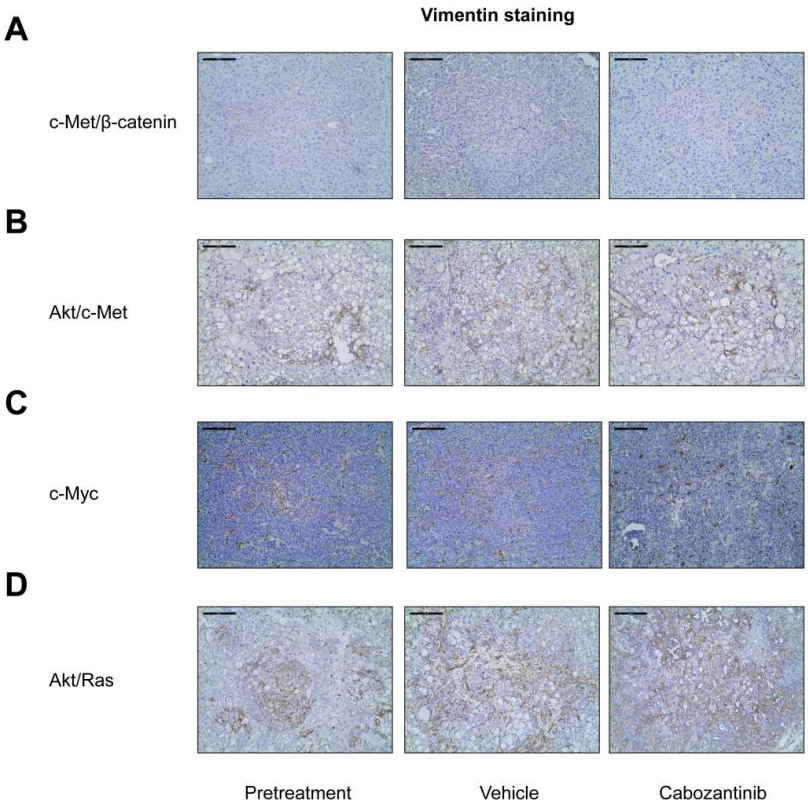

Supplementary Figure 17. Cabozantinib treatment does not affect cancer associated fibroblasts in mouse HCCs. Vimentin (magnification ×100; scale bar =200 μm) staining in livers from c-Met/β-Catenin **(A)**, Akt/c-Met **(B)**, c-Myc **(C)**, and Akt/Ras **(D)** mice.

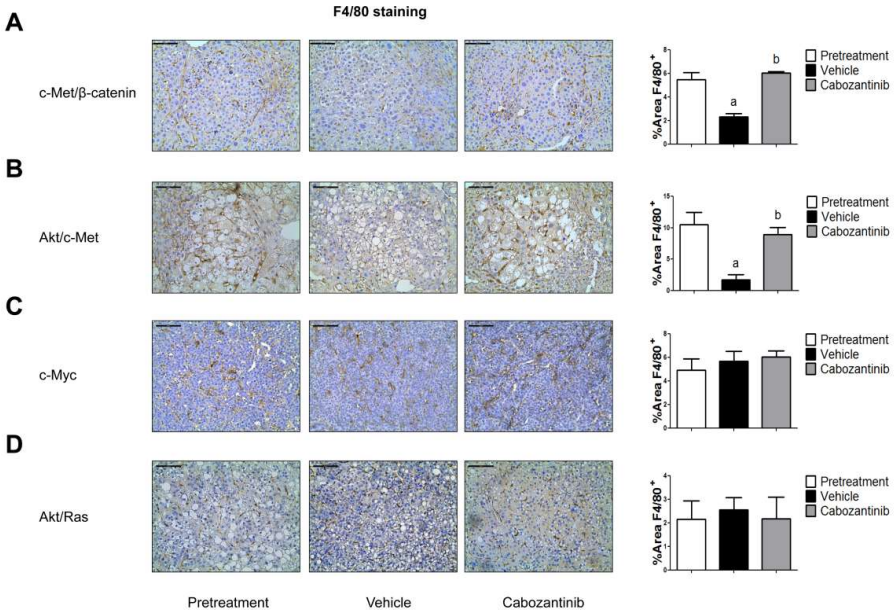

Supplementary Figure 18. Cabozantinib normalizes the presence of macrophages in c-Met/β-catenin and Akt/c-Met mouse HCC. F4/80 (magnification ×200; scale bar =100 μm) staining in livers from c-Met/β-Catenin **(A)**, Akt/c-Met **(B)**, c-Myc **(C)**, and Akt/Ras **(D)** mice. Student's t test: at least $P < 0.01$; a, vs. Pretreatment; b, vs. Vehicle.

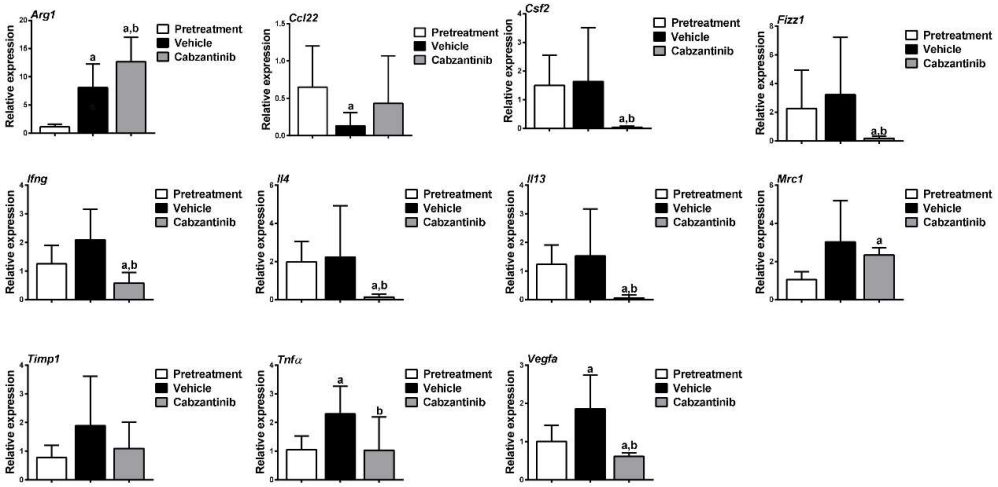

Supplementary Figure 19. Effect of Cabozantinib on macrophage polarization in the c-Met/β-Catenin model. Quantitative RT-PCR gene expression analysis of alternative macrophages prototypic markers in pretreatment, vehicle-, and Cabozantinib-treated c-Met/β-Catenin mice. Tukey–Kramer test: at least $P < 0.05$ a, vs Pretreatment; b, vs Vehicle; c, vs Cabozantinib.

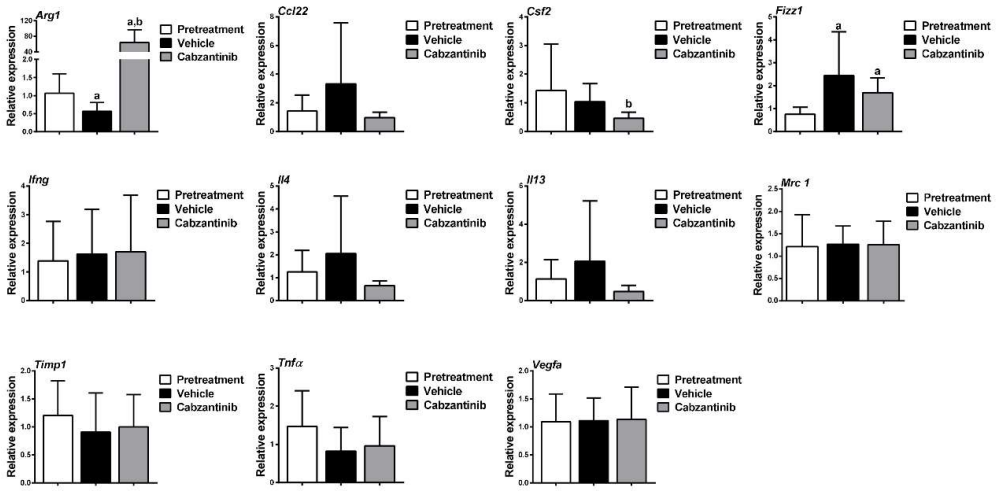

Supplementary Figure 20. Effect of Cabozantinib on macrophage polarization in the Akt/c-Met model. RT-qPCR gene expression analysis of alternative macrophages prototypic markers in pretreatment, vehicle-, and Cabozantinib-treated Akt/c-Met mice. Tukey–Kramer test: at least $P < 0.05$ a, vs Pretreatment; b, vs Vehicle; c, vs Cabozantinib.

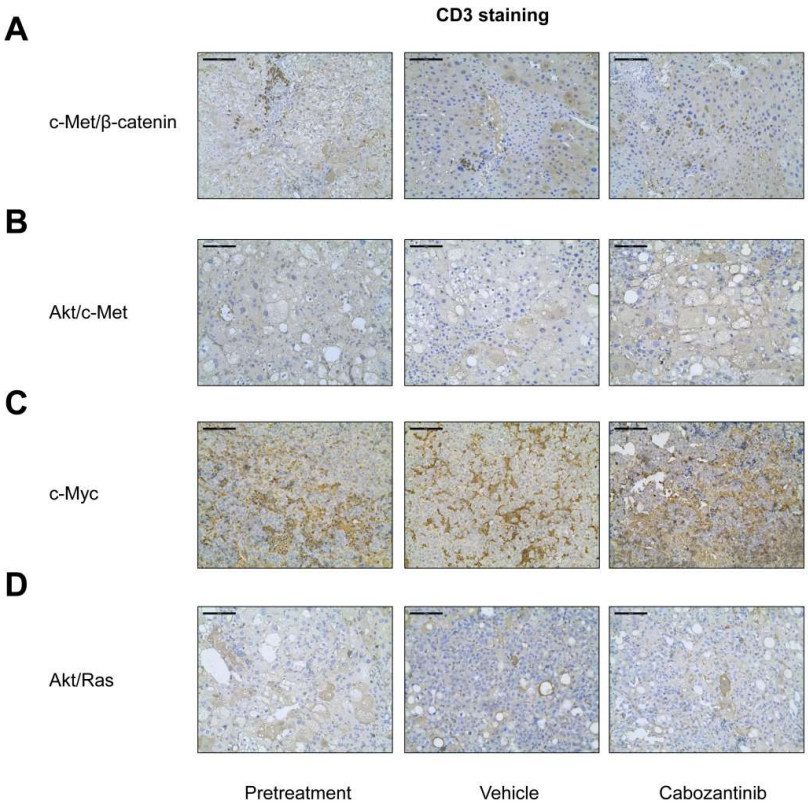

Supplementary Figure 21. Cabozantinib treatment does not affect CD3(+) T lymphocytes in mouse HCCs. CD3 (magnification ×200; scale bar =100 μm) staining in livers from c-Met/β-Catenin **(A)**, Akt/c-Met **(B)**, c-Myc **(C)**, and Akt/Ras **(D)** mice.

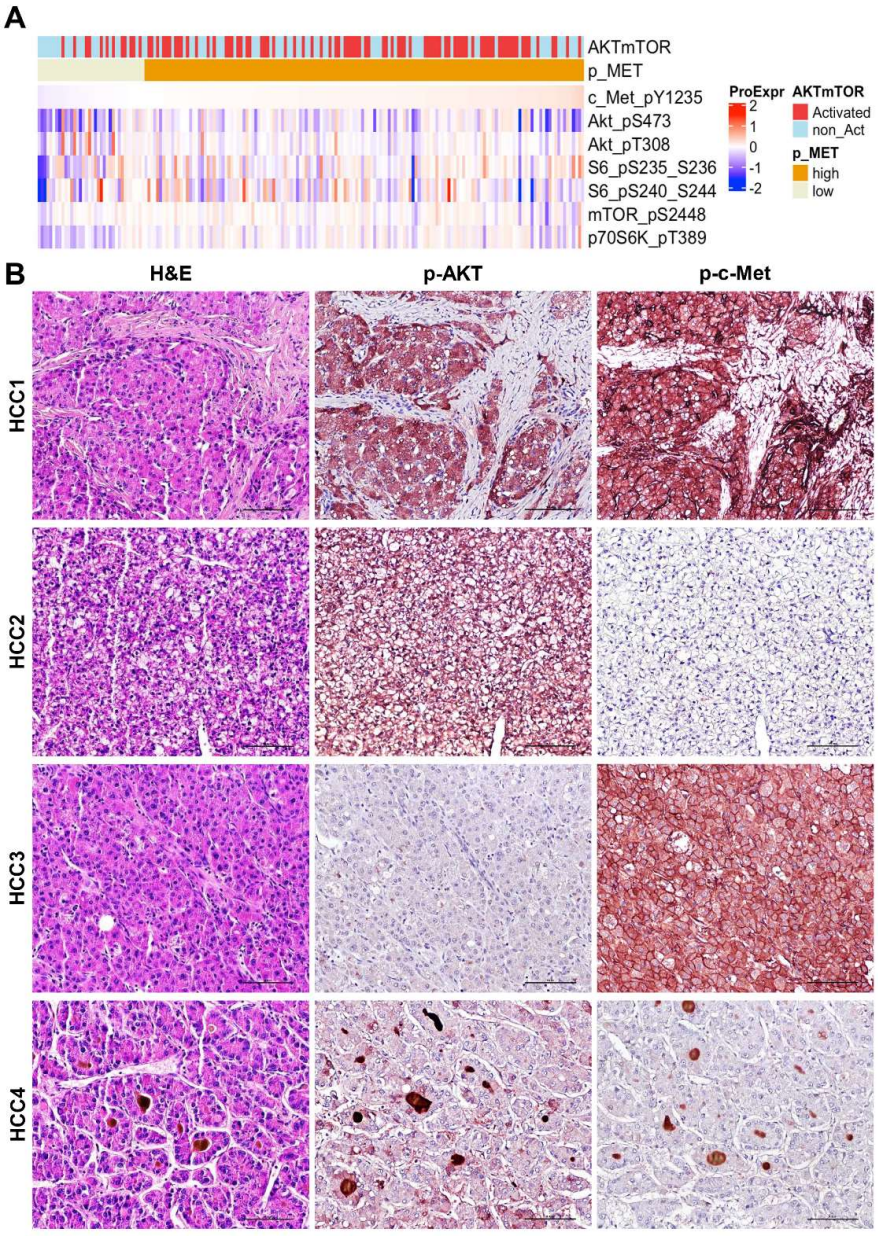

Supplementary Figure 22. Relationship of AKT and c-MET activation in human HCC. (A) Heatmap of the human TCGA samples depicting AKT/mTOR pathway activation and inferred c-MET activation. **(B)** Immunohistochemical patterns for activated/phosphorylated p-AKT and activated/phosphorylated p-MET in human hepatocellular carcinoma (HCC) specimens (n=64). Four HCC staining patterns are

shown in four HCC samples (HCC1-4). Specifically, HCC1 exhibits concomitant induction of p-AKT and p-c-MET; HCC2 shows elevated immunoreactivity for p-AKT, whereas HCC3 displays immunoreactivity only for p-c-MET. No immunoreactivity for p-AKT and p-c-MET is appreciable in HCC4. Higher immunoreactivity for p-AKT and p-c-MET was detected in 38 of 64 (59.4%) and 25 of 64 (39.06%) HCC specimens, respectively. Also, 21 of 64 (32.81%) HCC specimens exhibited concomitantly elevated p-AKT and p-c-MET immunoreactivity. The orange staining in the three panels of HCC4 indicates the presence of bile deposits within the tumor. Original magnification: 200x; scale bar: 100 μm. Abbreviation: H&E, hematoxylin and eosin staining.

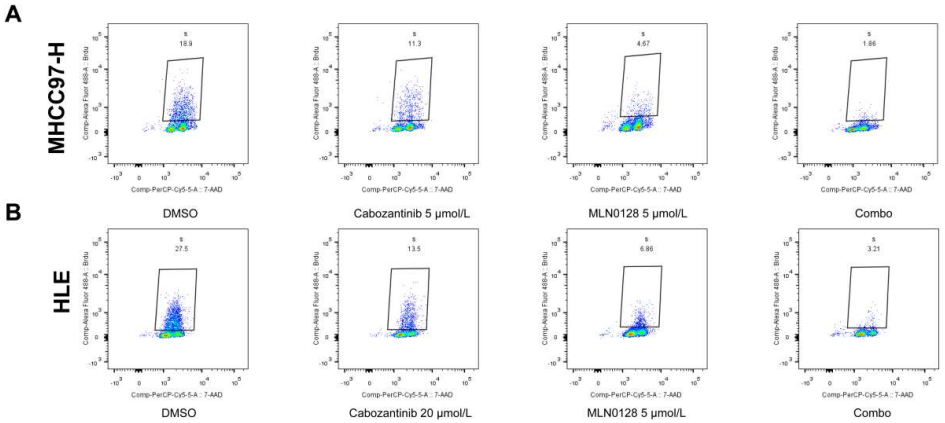

Supplementary Figure 23. Effects of combined Cabozantinib/MLN0128 treatment on the cell cycle. (A and B) Combined Cabozantinib with MLN0128 resulted in enhanced cell cycle arrest in MHCC97-H and HLE cell lines. Abbreviations: Combo, combined Cabozantinib/MLN0128 treatment.

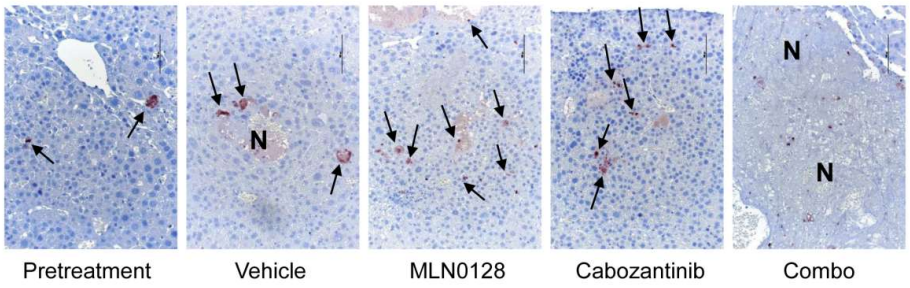

Supplementary Figure 24. Cabozantinib and MLN0128 combination (Combo) induces apoptosis and necrosis in HCC from c-Met/β-Catenin mice. TUNEL staining (magnification ×200; scale bar =100 μm) of liver lesions from c-Met/β-Catenin mice. While either Cabozantinib or MLN0128 treatment significantly increased apoptosis when compared with vehicle and pretreatment groups, large areas of the tumors were replaced by necrosis (N) and extensive apoptosis following administration of the two drugs together. Arrows indicate apoptotic cells. Abbreviations: Combo, Cabozantinib and MLN0128 combination; N, necrosis.

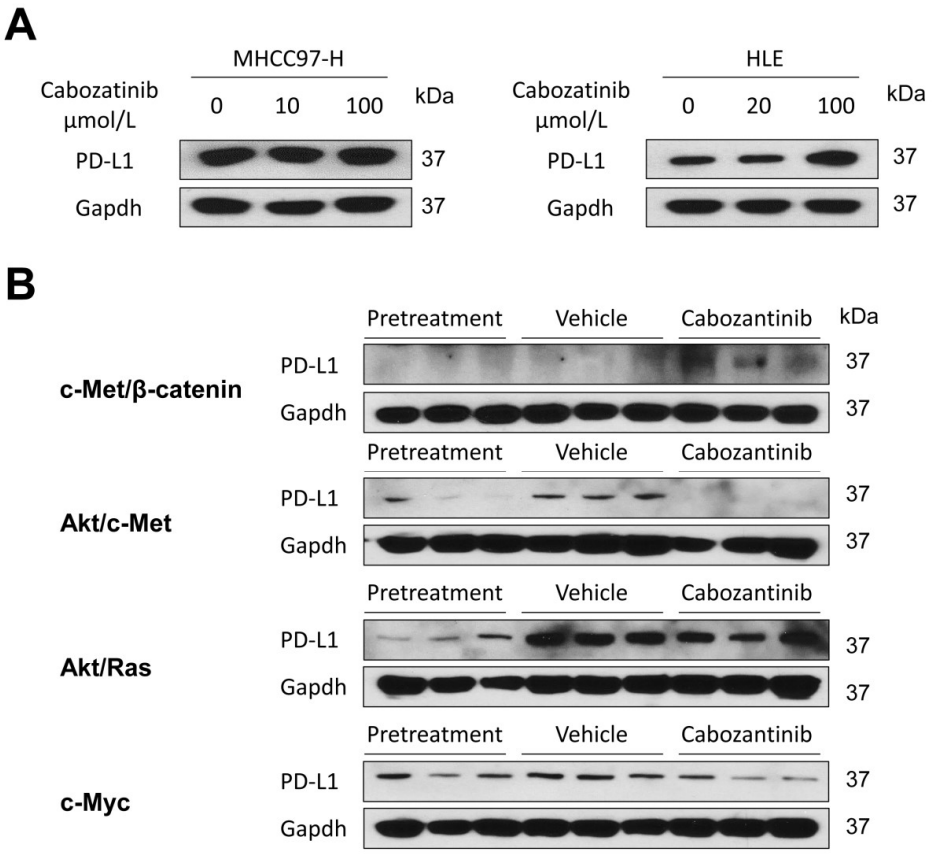

Supplementary Figure 25. Effects of Cabozantinib on PD-L1 expression in HCC cells and mouse HCCs. Representative images of Western blot analysis from HCC cell lines **(A)** and mouse HCC samples **(B).**

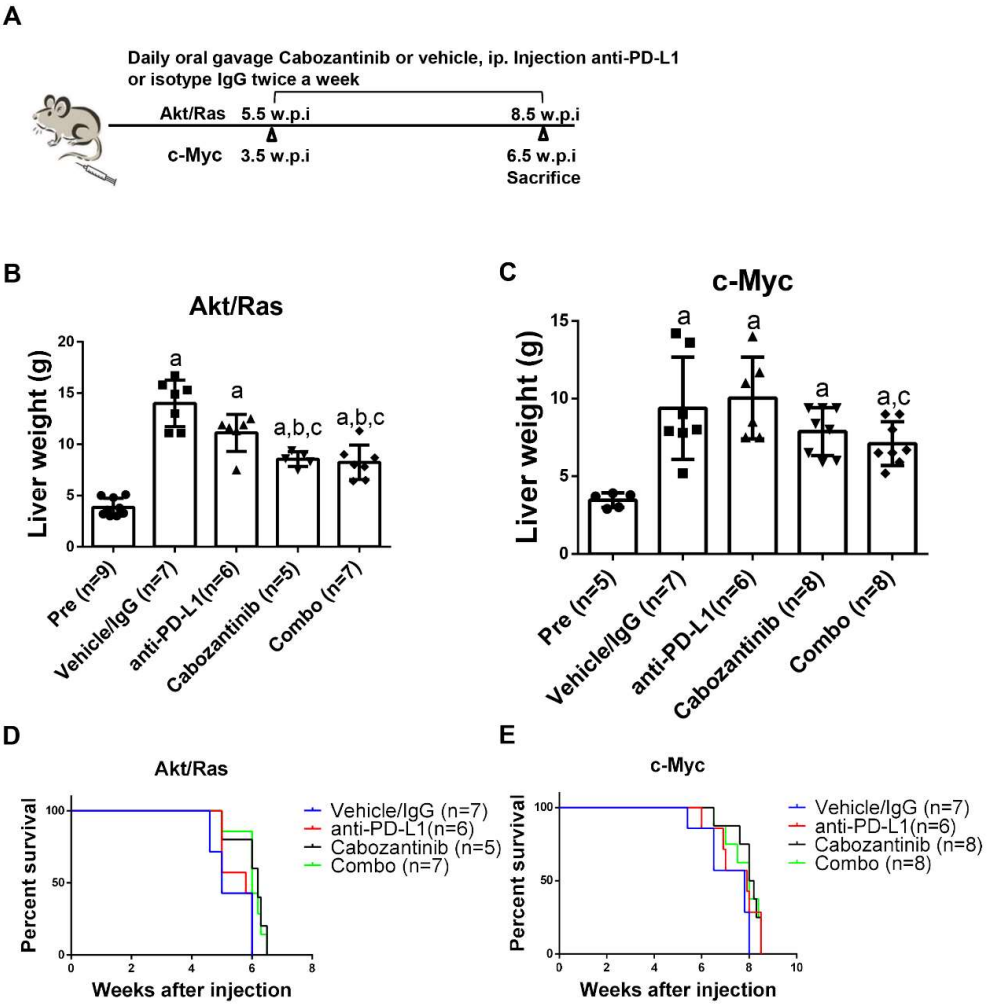

Supplementary Figure 26. Effect of combined Cabozantinib and anti-PD-L1 treatment in Akt/Ras mice and c-Myc mice. (A) Study design. Liver weight of pretreatment-, vehicle/isotype IgG -, Cabozantinib-, PD-L1- and Cabozantinib/anti-PD-L1-treated Akt/Ras mice **(B)**, and c-Myc mice **(C).** Survival curve of in Akt/Ras mice **(D)** and c-Myc mice **(E)** treated with vehicle/isotype IgG, Cabozantinib, PD-L1 and Cabozantinib/anti-PD-L1. Tukey–Kramer test: at least $P < 0.05$. a, vs. Pretreatment; b, vs. Vehicle; c, vs. anti-PD-L1. Abbreviations: Pre, Pretreatment; Cabo, Cabozantinib; Comb, combined Cabozantinib and anti-PD-L1 treatment.

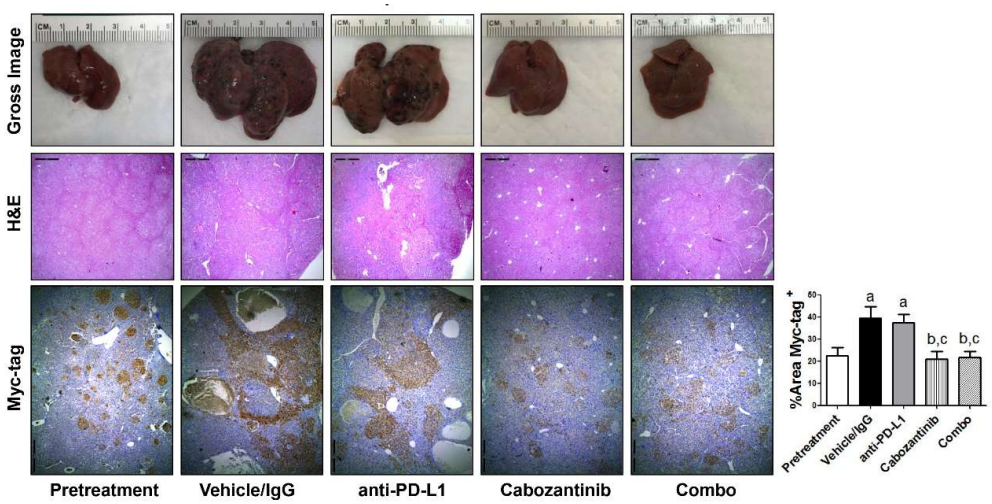

Supplementary Figure 27. Morphology and histology of Cabozantinib/PD-L1 Ab treated c-Met/β-Catenin mice. Gross images and H&E, Myc-tag staining (magnification ×40; scale bar =500 μm) of livers from Pretreatment, Vehicle/Isotype IgG-treated, anti-PD-L1-treated, Cabozantinib-treated and Cabozantinib/PD-L1-treated c-Met/β-Catenin mice**.** Combo, combined Cabozantinib/anti-PD-L1 treatment.

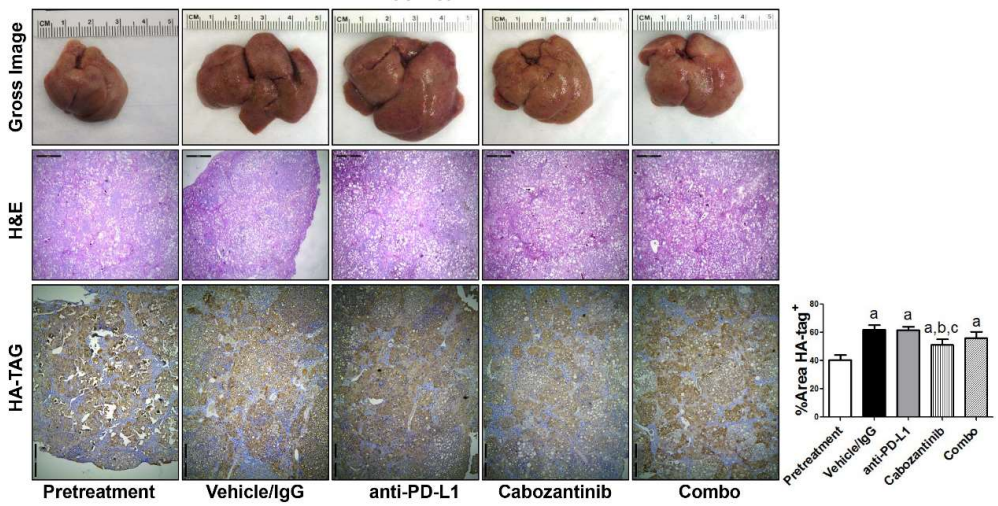

Supplementary Figure 28. Morphology and histology of Cabozantinib/PD-L1 Ab treated Akt/c-Met mice. Gross images and H&E, HA-TAG staining (magnification ×40; scale bar =500 μm) of livers from Pretreatment, Vehicle/Isotype IgG-treated, anti-PD-L1-treated, Cabozantinib-treated and Cabozantinib/PD-L1-treated Akt/c-Met mice**.** Combo, combined Cabozantinib/anti-PD-L1 treatment.

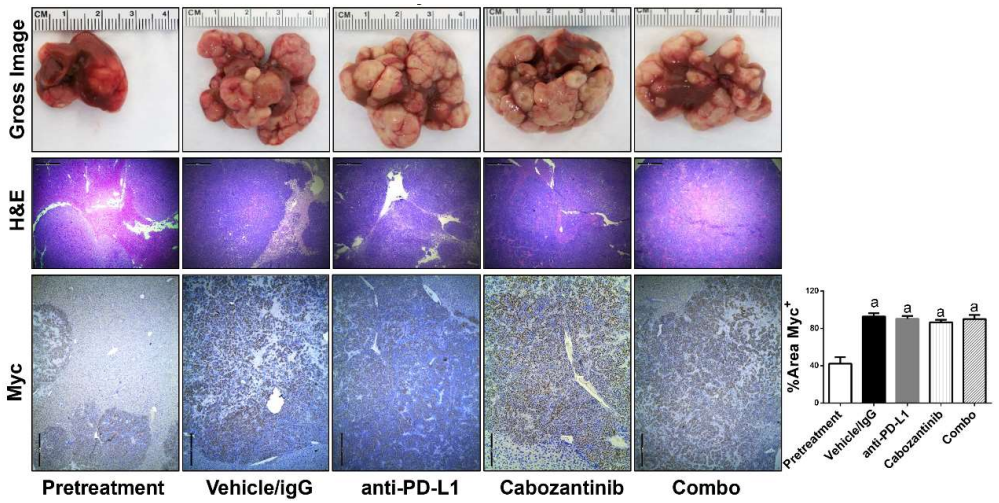

Supplementary Figure 29. Morphology and histology of Cabozantinib/PD-L1 Ab treated Myc mice. Gross images and H&E, Myc staining (magnification ×40; scale bar =500 μm) of livers from Pretreatment, Vehicle/Isotype IgG-treated, anti-PD-L1-treated, Cabozantinib-treated and Cabozantinib/PD-L1-treated Akt/c-Met mice. Combo, combined Cabozantinib/anti-PD-L1 treatment.

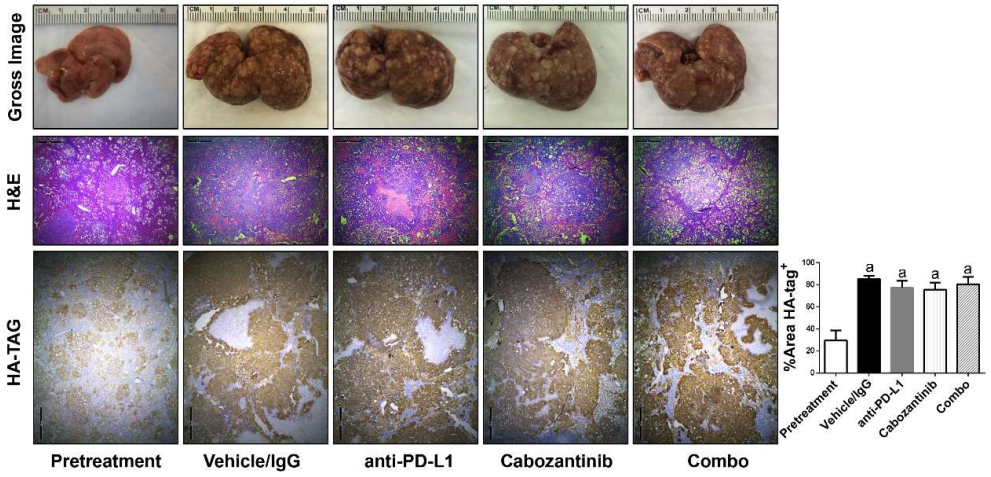

Supplementary Figure 30. Morphology and histology of Cabozantinib/PD-L1 Ab treated Akt/Ras mice. Gross images and H&E, HA-TAG staining (magnification ×40; scale bar =500 μm) of livers from Pretreatment, Vehicle/Isotype IgG-treated, anti-PD-L1-treated, Cabozantinib-treated and Cabozantinib/PD-L1-treated c-Met/β-Catenin mice. Combo, combined Cabozantinib/anti-PD-L1 treatment.

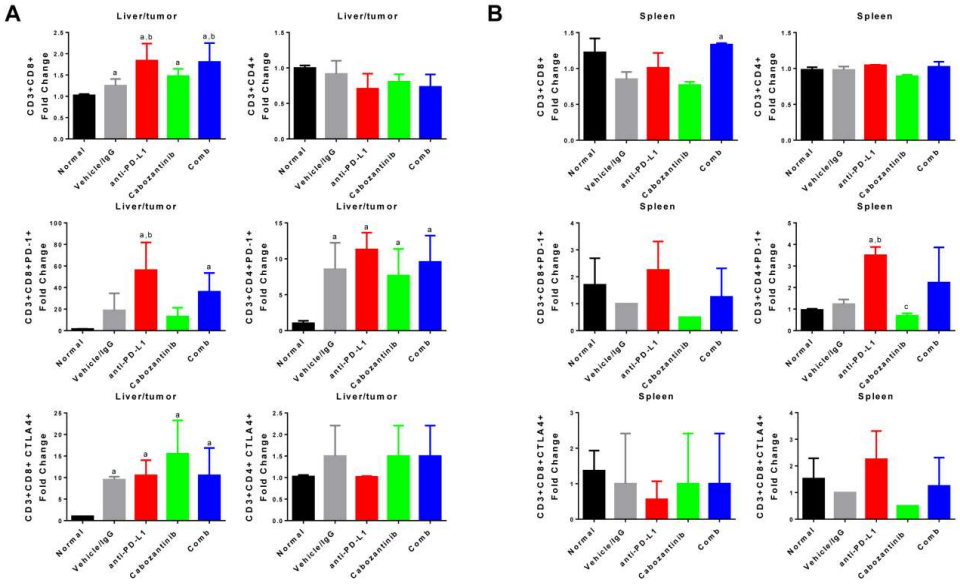

Supplementary Figure 31. Immune response in Cabozantinib/PD-L1 Ab treated c-Met/β-Catenin mice. Cell suspensions from liver/tumor **(A)** and spleen **(B)** of tumor-free mice, c-Met/β-Catenin tumor-bearing mice were stained for CD3, CD4, CD8, PD-1 and CTLA-4 and analyzed by flow cytometry. Tukey–Kramer test: at least $P < 0.05$. a, vs. Normal; b, vs. Vehicle. Abbreviations: Normal, tumor-free mice; Combo, combined Cabozantinib/anti-PD-L1 treatment.

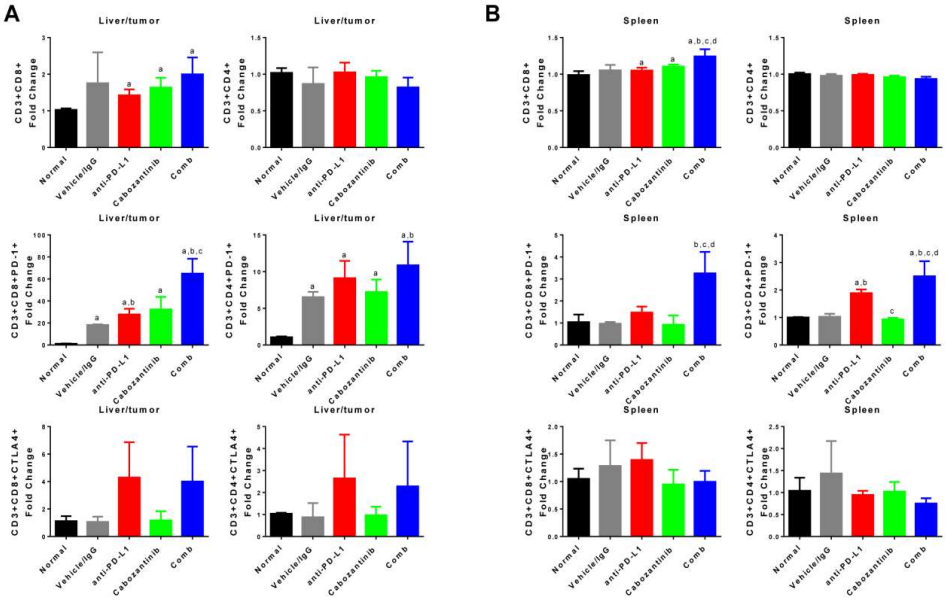

Supplementary Figure 32. Immune response in Cabozantinib/PD-L1 Ab treated Akt/c-Met mice. Cell suspensions from liver/tumor **(A)** and spleen **(B)** of tumor-free mice, AKT/c-Met tumor-bearing mice were stained for CD3, CD4, CD8, PD-1 and CTLA-4 and analyzed by flow cytometry. Tukey–Kramer test: at least $P < 0.05$. a, vs. Normal; b, vs. Vehicle. Abbreviations: Normal, tumor-free mice; Combo, combined Cabozantinib/anti-PD-L1 treatment.

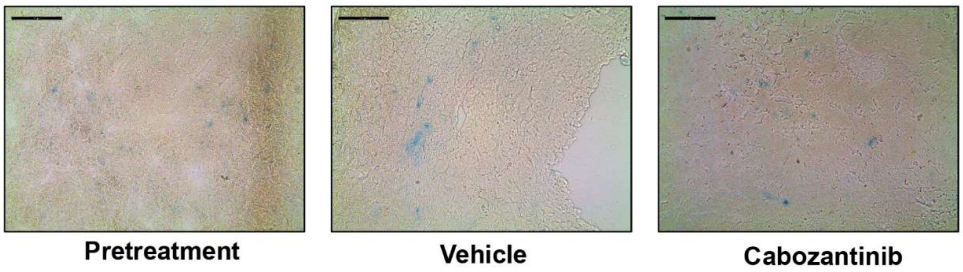

Supplementary Figure 33. Senescence detection in Cabozantinib treated c-Met/β-catenin mice. Original magnification: 200x; scale bar: 100 μm.

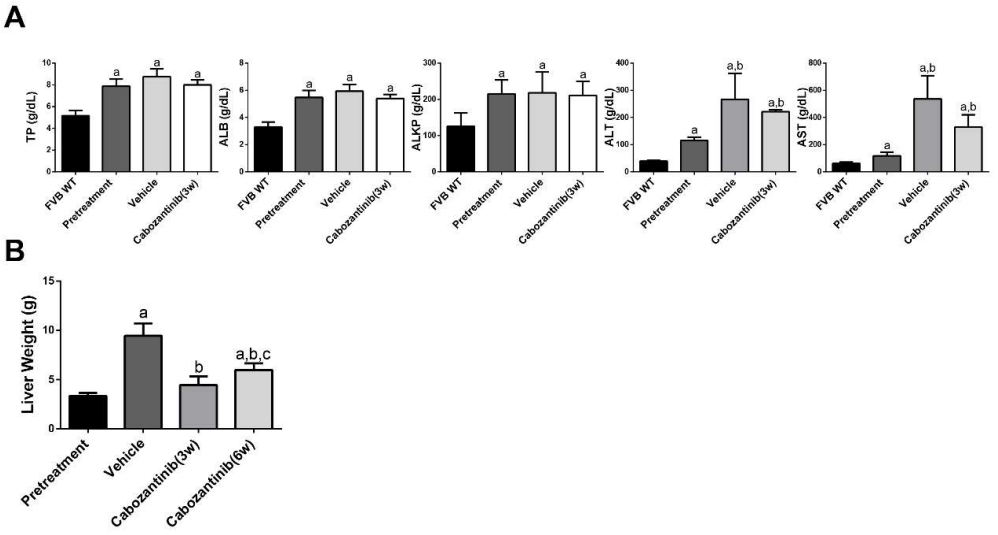

Supplementary Figure 34. The efficacy of Cabozantinib short-term and long-term treatment in c-Met/β-catenin mice. (A) Indicators of liver function in c-Met/β-catenin mice treated with Cabozantinib (3 weeks). **(B)** Liver weight of Vehicle- or 60mg/kg/day Cabozantinib-treated (3 weeks and 6 weeks) c-Met/β-catenin mice. Tukey–Kramer test: at least $P < 0.05$; a, vs. Pretreatment; b, vs. Vehicle; c, vs. Cabozantinib (3w). Abbreviations: ALT, alanine aminotransferase; AST, aspartate aminotransferase; TBIL, total bilirubin; DBIL, direct bilirubin; TP, total protein; ALB, albumin; 3w, 3 weeks; 6w, 6 weeks. At least 3 mice per group.

Supplementary Table 1. List of antibodies used for immunohistochemistry

Antibody	Catalog number	Company	Species	Dilution
Ki-67	MA5-14520	Thermo Fisher scientific	Rabbit	1:150
Myc-tag	2278	Cell Signaling Technology	Rabbit	1:100
Phospho-p44/42 MAPK (Erk1/2) (Thr202/Tyr204)	4370	Cell Signaling Technology	Rabbit	1:100
Phospho-Akt (Ser473) for mice tissue	4060	Cell Signaling Technology	Rabbit	1:100
Phospho-Akt (Ser473) for human tissue	66444-1-Ig	Proteintech	Mouse	1:100
Phospho-Met (Tyr1234/1235)	3077	Cell Signaling Technology	Rabbit	1:100
CD34	ab81289	Abcam	Rabbit	1:2500
CD31	77699	Cell Signaling Technology	Rabbit	1:100
F4/80	14-4801-82	eBioscience	Rat	1:100
CD3	sc-20047	Santa Cruz Biotechnology	Mouse	1:50
Vimentin	5741	Cell Signaling Technology	Rabbit	1:200

Supplementary Table 2. List of antibodies used for Western blot analysis

Antibody	Catalog number	Company	Species	Dilution
GAPDH	5174	Cell Signaling Technology	Rabbit	1:2000
β-Actin	A5441	Sigma-Aldrich	Mouse	1:5000
c-Met	71-8000	Invitrogen	Rabbit	1:400
c-Met	ab59884	Abcam	Mouse	1:150
Phospho-Met (Tyr1234/1235)	3077	Cell Signaling Technology	Rabbit	1:200
β-Catenin	Bd 610153	BD Biosciences	Mouse	1:2000
Vegfr2	2479	Cell Signaling Technology	Rabbit	1:1000
Phospho-Vegfr2 (Tyr1054/1059)	ab5473	Abcam	Rabbit	1:1000
Axl	8661	Cell Signaling Technology	Rabbit	1:100
Phospho-Axl (Tyr702)	5724	Cell Signaling Technology	Rabbit	1:100
Stat3	ab68153	Abcam	Rabbit	1:1000
Phospho-Stat3 (Tyr705)	9145	Cell Signaling Technology	Rabbit	1:1000
Phospho-Akt (Ser473)	4060	Cell Signaling Technology	Rabbit	1:1000
Akt	9272	Cell Signaling Technology	Rabbit	1:1000

p44/42 MAPK (Erk1/2)	9102	Cell Signaling Technology	Rabbit	1:1000
Phospho-p44/42 MAPK (Erk1/2) (Thr202/Tyr204)	4370	Cell Signaling Technology	Rabbit	1:1000
Phospho-mTOR (Ser2481)	2974	Cell Signaling Technology	Rabbit	1:1000
mTOR	2983	Cell Signaling Technology	Rabbit	1:1000
Phospho-4EBP1 (Ser65)	9451	Cell Signaling Technology	Rabbit	1:2000
4EBP1	9644	Cell Signaling Technology	Rabbit	1:2000
Phospho-S6 Ribosomal Protein	4858	Cell Signaling Technology	Rabbit	1:1000
S6 Ribosomal Protein	2217	Cell Signaling Technology	Rabbit	1:1000
PCNA	2586	Cell Signaling Technology	Mouse	1:2000
Survivin	2808	Cell Signaling Technology	Rabbit	1:1000
Cleaved Caspase-3	9664	Cell Signaling Technology	Rabbit	1:1000
Cyclin A	sc-751	Santa Cruz Biotechnology	Rabbit	1:200
Cyclin D1	ab134175	Abcam	Rabbit	1:10000

Cyclin E	sc-481	Santa Cruz Biotechnology	Rabbit	1:200
p16	ab51243	Abcam	Rabbit	1:200
p21	556430	BD	Mouse	1:200
p27	610242	BD Biosciences	Mouse	1:1000
p53	sc-126	Santa Cruz Biotechnology	Mouse	1:200
Phospho-Rb (Ser780)	9307	Cell Signaling Technology	Rabbit	1:500
HIF-1α	14179	Cell Signaling Technology	Rabbit	1:500
PDHA	3205	Cell Signaling Technology	Rabbit	1:1000
LDHA/LDHC	3558	Cell Signaling Technology	Rabbit	1:1000
PKM1	7067	Cell Signaling Technology	Rabbit	1:1000
PKM2	4053	Cell Signaling Technology	Rabbit	1:1000
Hexokinase 2	2867	Cell Signaling Technology	Rabbit	1:1000
Acetyl-CoA Carboxylase	3676	Cell Signaling Technology	Rabbit	1:5000
Fatty Acid Synthase	3180	Cell Signaling Technology	Rabbit	1:2000

SCD1	2794	Cell Signaling Technology	Rabbit	1:500
PD-L1	NBP1-76769	Novus Biologicals	Rabbit	1:1000

Supplementary Table 3. List of antibodies used for flow cytometric analysis.

Antibody	Company	Catalog number
CD3-FITC	Biolegend	100203
CD4-PE	Biolegend	100407
CD8-BV605	Biolegend	100743
PD1-BV421	Biolegend	135217
CTLA4-APC	Biolegend	106309